PRODUCTION OF NEUTRON-RICH ISOTOPES IN THE CALCIUM REGION

O.B.TARASOV[1,*], D.J. MORRISSEY[1,2], A.M.AMTHOR[3], L. BANDURA[3], T.BAUMANN[1], D.BAZIN[1], J.S. BERRYMAN[1], G.CHUBARIAN[4], N FUKUDA[5], A.GADE[1,6], T.N.GINTER[1], M. HAUSMANN[3], N. INABE[5], T.KUBO[5], J.PEREIRA[1], M. PORTILLO[3], B.M.SHERRILL[1,6], A. STOLZ[1,6], C.SUMITHRARACHCHI[1], M. THOENNESSEN[1,6], D. WEISSHAAR[1]

[1] *National Superconducting Cyclotron Laboratory, Michigan State Univ., MI 48824, USA*

[2] *Department of Chemistry, Michigan State University, East Lansing, MI 48824, USA*

[3] *Facility for Rare Isotope Beams, Michigan State Univ., East Lansing, MI 48824, USA*

[4] *Cyclotron Institute, Texas A&M University, College Station, TX 77843, USA*

[5] *RIKEN Nishina Center, RIKEN, Wako-shi, Saitama 351-0198, Japan*

[6] *Dep. of Physics and Astronomy, Michigan State Univ., East Lansing, MI 48824, USA*

Production cross sections for neutron-rich nuclei from the fragmentation of a ^{82}Se beam at 139 MeV/u were measured. The longitudinal momentum distributions of 122 neutron-rich isotopes of elements $11 \leq Z \leq 32$ were determined by varying the target thickness. Production cross sections with beryllium and tungsten targets were determined for a large number of nuclei including several isotopes for the first time observed in this work. These are the most neutron-rich nuclides of the elements $22 \leq Z \leq 25$ (^{64}Ti, ^{67}V, ^{69}Cr, ^{72}Mn). One event was registered consistent with ^{70}Cr, and another one with ^{75}Fe. A one-body Q_g systematics is used to describe the production cross sections based on thermal evaporation from excited prefragments. The current results confirm those of our previous experiment with a ^{76}Ge beam: a change in the nuclear mass surface near $Z = 20$.

* On leave from Flerov Laboratory of Nuclear Reactions, JINR, 141980 Dubna, Moscow Region, Russian Federation

1. Introduction

The discovery of new nuclei in the proximity of the neutron dripline provides a test for nuclear mass models, and hence for the understanding of the nuclear force and the creation of elements. Once neutron-rich nuclei are observed, and their cross sections for formation are understood, investigations to study the nuclei themselves, such as decay spectroscopy, can be planned. Therefore, obtaining production rates for the most exotic nuclei continues to be an important part of the experimental program at existing and future rare-isotope facilities.

Progress in the production of neutron-rich isotopes was made possible by the increase of primary beam intensities, new beam development at the National Superconducting Cyclotron Laboratory (NSCL) at Michigan State University and advances in experimental techniques [3]. Indeed, recent measurements at the NSCL [1-5] have demonstrated that the fragmentation of ^{48}Ca and ^{76}Ge beams can be used to produce new isotopes in the proximity of the neutron dripline. Continuing this work, we report here the next step with a newly developed ^{82}Se beam towards the fundamental goal of defining the absolute mass limit for chemical elements in the region of calcium.

One of the first indications of significant changes in the structure of neutron rich nuclei was the discovery of enhanced nuclear binding of heavy sodium isotopes [6]. This is now understood to result from significant contributions of *fp* shell intruder orbitals to the ground-state configurations of these isotopes [7,8]. Low-lying 2+ states and quadrupole collectivity have been reported in neutron-rich even-even Ne and Mg isotopes around $N = 20$, see for example Refs. [9,10]. This region around ^{31}Na, where the neutron *fp* shell contributes significantly to the ground-state structure, is now known as the "Island of Inversion". Similarly, there is mounting evidence for an onset of deformation around neutron number $N = 40$ in Fe and Cr nuclei. Neutron $g_{9/2}$ and $d_{5/3}$ configurations from above the $N = 40$ shell gap are proposed to descend and dominate the low-lying configurations similar to the $N = 20$ Island of Inversion [11,12].

Recently, it was shown that the beta-decay half-lives of the neutron-rich Ca isotopes compare [13] favorably with the results of shell-model calculations performed in the full *pf* model space using the GXPF1 effective interaction [14]. The systematic trend of these half-lives is consistent with the presence of a subshell gap at $N = 32$ as predicted by this interaction and as was confirmed by experiments. This interaction also predicts an increase of $E_x(2_1^+)$ at ^{54}Ca, suggesting the appearance of the $N = 34$ shell gap in Ca isotopes.

In our previous cross section measurements in the region around ^{62}Ti (^{76}Ge primary beam) [2] we observed a systematic smooth variation of the production cross sections that might point to nuclear structure effects, for example, an onset of collectivity, that are not included in global mass models that form the basis of systematics. The present work, since using a different primary beam, provides an independent check of this interpretation.

2. Experiment

A newly developed 139 MeV/u ^{82}Se beam with an intensity of 35 pnA, accelerated by the coupled cyclotrons at the NSCL, was fragmented on a series of beryllium targets and a tungsten target, each placed at the object position of the A1900 fragment separator [15]. In this work we used an identical configuration as in our previous experiment with a ^{76}Ge beam [1], where the combination of the A1900 fragment separator with the S800 analysis beam line [16] formed a two-stage separator system that allowed a high degree of rejection of unwanted reaction products. At the end of the S800 analysis beam line, the particles of interest were stopped in a telescope of eight silicon PIN diodes (50×50 mm^2) with a total thickness of 8.0 mm. A 50 mm thick plastic scintillator positioned behind the Si-telescope served as a veto detector against reactions in the Si-telescope and provided a measurement of the residual energy of lighter ions that were not stopped in the Si-telescope. A position sensitive parallel plate avalanche counter (PPAC) was located in front of the Si-telescope. All experimental details and a sketch of the experimental setup can be found in Ref. [1].

In order to the search for new isotopes, five settings were used to cover the most neutron-rich isotopes with $20 \leq Z \leq 27$, as it was impossible to find a single target thickness and magnetic rigidity to produce all of the fragments of interest. Each setting was characterized by a fragment for which the separator was tuned. A search for the most exotic nuclei in each setting was carried out with Be and W targets. The settings were centered on ^{60}Ca, ^{68}V and ^{74,75}Fe respectively, based on LISE^{++} [17] calculations using the parameterizations of the momentum distributions obtained in the first part of the experiment. The momentum acceptance of the A1900 was set to the maximum of $\Delta p/p$ = 5.0% for these production runs.

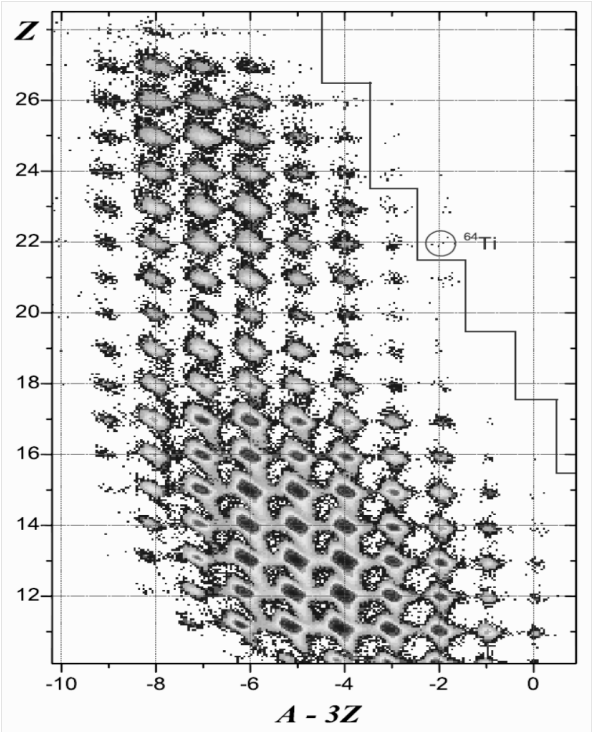

Figure 1. Particle identification plot showing the measured atomic number, *Z*, versus the calculated function *A* - 3*Z* for the nuclei observed in production runs of this work. See text for details. The limit of previously observed nuclei is shown by the solid red line as well as the locations of a reference nucleus (^{64}Ti).

The particle identification matrix of fully-stripped reaction products observed in the production runs is shown in Fig.1. The range of fragments is shown as a function of the measured atomic number, *Z*, versus the calculated quantity $A - 3Z$. The identification of the individual isotopes was confirmed via isomer tagging using the known isomeric decays in ^{67}Fe and ^{78}Zn. The standard deviations of ionic (q) and elemental (Z) spectra were found to be similar to those in the previous experiment, therefore the probabilities of one event being misidentified as a neighboring charge state or element were as small as before. The details of the calculation of the particle identification are given in the appendix of the previous work [1]. The observed fragments include several new isotopes that are the most neutron-rich nuclides yet observed of elements

$22 \leq Z \leq 25$ (^{64}Ti, ^{67}V, ^{69}Cr, ^{72}Mn). One event was found to be consistent with ^{70}Cr, and another one with ^{75}Fe. The new neutron-rich nuclei observed in this work are those events to the right of the solid line in Fig.1.

3. Results and Discussion

3.1. *Momentum distributions*

The prediction of the momentum distributions of residues is important when searching for new isotopes in order to set the fragment separator at the maximum production rate. Also, the accurate prediction of the momentum distributions allows a precise estimate of the transmission and efficient rejection of strong contaminants. In this experiment the "target scanning" approach [18] developed in the previous experiment was used to obtain parameters for the neutron-rich isotope momentum distribution models such as [19,20]. This method is particularly well suited to survey neutron-rich nuclei since the less exotic nuclei are produced with the highest yields and their momentum distributions can be measured with the thin targets.

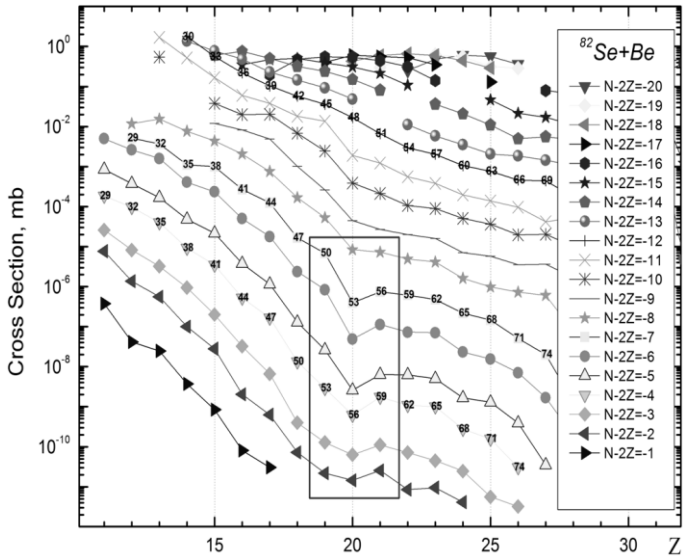

Figure 2. Production cross sections for fragments from the reaction of ^{82}Se with beryllium targets vs. the atomic number of the fragment. The cross sections are connected by lines of constant *N*-2*Z*. The red rectangle highlights a possible region of structural change for the calcium isotopes with mass numbers 53-56.

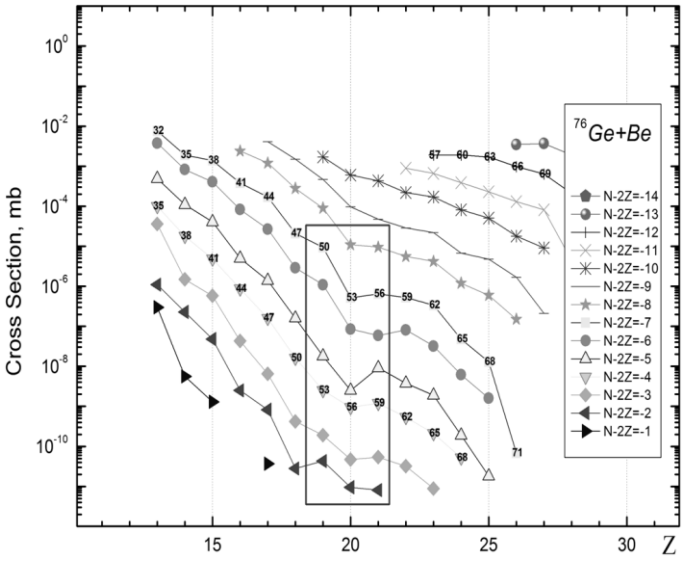

Figure 3. Similar to Fig.2 for data with the ^{76}Ge primary beam [1].

The data analysis of this approach has been updated, and a detailed explanation is in preparation [21]. Important improvements include: first, that the most probable velocity for a fragment is not that at the center of the target if the yield is sharply rising or falling with momentum, and second, asymmetric Gaussian distributions have been used where the asymmetry coefficients have been taken from the convolution model implemented in the LISE^{++} code [17]. Note that, at the energy of these experiments, the shape of the fragment momentum distribution is slightly asymmetric with a low-energy exponential tail stemming from dissipative processes [22]. Seven targets were used to measure the momentum distributions. The momentum distributions for 122 isotopes were derived and integrated to deduce the production cross sections. A survey of all of the fitted results showed that neutron-rich fragments were produced with significantly higher velocities than the momentum distribution models [20,23] predict, and this result is similar to our previous measurements [18].

3.2. *Production cross section*

The inclusive production cross sections for the observed fragments were calculated by correcting the measured yields for the finite momentum and angular acceptances of the separator system. The cross sections for all of the

remaining fragments with incompletely measured longitudinal momentum distributions were obtained with estimated transmission corrections as has been done in our previous work [1]. The angular and momentum transmissions were calculated for each isotope in each setting using a model of the momentum distribution with smoothly varying parameters extracted from the measured parallel momentum distributions.

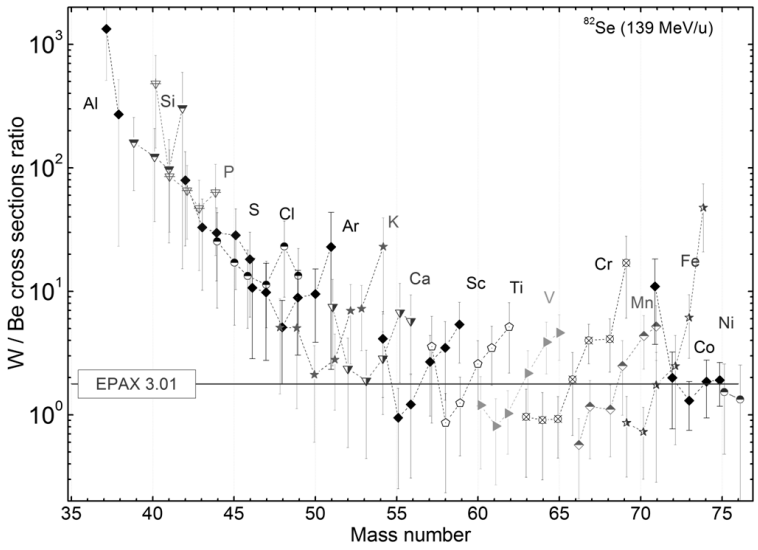

Figure 4. Target ratios of the production cross sections $\sigma_W(A,Z)$ / $\sigma_{Be}(A,Z)$ of fragments $13 \le Z \le 28$ for the ^{82}Se projectile. The horizontal solid line indicates the ratio calculated by the EPAX 3 formula [24].

The cross sections obtained in the experiment with beryllium targets are shown in Fig.2. This representation with $N - 2Z$ lines highlights a significant suppression of the production cross sections for calcium isotopes with mass numbers 53-56. The same trend for this region (see Fig.3) has been observed as well with the ^{76}Ge primary beam [1]. There are advantages using a heavy target to produce neutron-rich isotopes of light elements, and a light target for heavier elements. This can be seen from Fig.4, where shown are the tungsten and beryllium target ratios of the production cross sections using the ^{82}Se projectile. It is necessary to note regarding to this figure, that isotopes of elements $17 \le Z \le 19$ have been observed for the first time using the W-target in the previous experiment with the ^{76}Ge primary beam [1], for isotopes with $20 \le Z \le 26$ accordingly with Be targets in this experiment (using the ^{82}Se beam), and in the previous with the ^{76}Ge beam.

The production cross sections for the most neutron-rich projectile fragments have been previously shown to have an exponential dependence on Q_g (the difference in mass-excess of the beam particle and the observed fragment) [2,4]. To test this behavior, the cross sections for each isotopic chain were fitted with the simple expression:

$$\sigma(Z, A) = f(Z) \exp(Q_g^*/T), \quad (1)$$

where T is an effective temperature or inverse slope. In this work neutron odd-even corrections have been applied for Q_g of neutron-odd isotopes, that do not change slopes of lines, but smooth the data and significantly decreases the χ^2-value. This correction has a large effect on the stable isotopes, and practically no influence for very exotic nuclei with weakly bound neutrons.

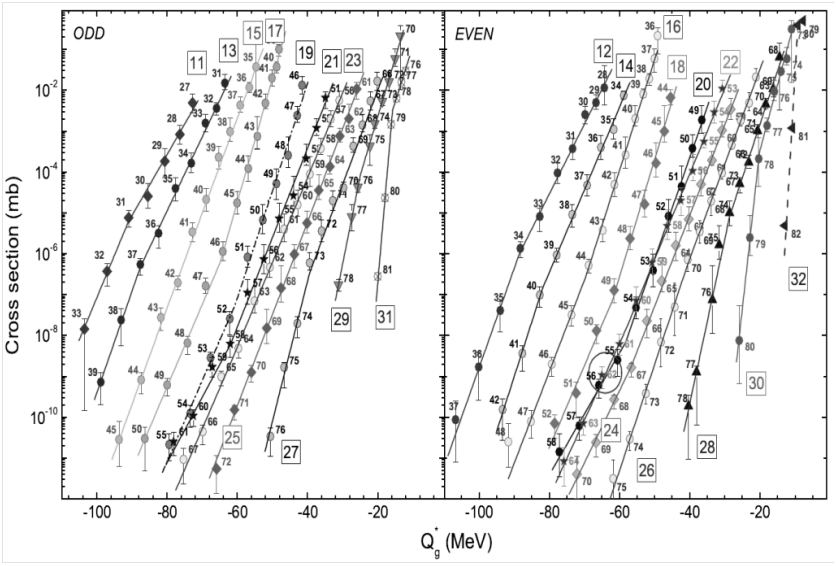

Figure 5. Cross sections for the production of neutron-rich nuclei with odd (left plot) and even (right plot) atomic numbers, with a beryllium target. See text for explanation of Q_g and the lines. The cross section for ^{62}Ti at the center of the proposed new island of inversion [11] are circled.

Fig.5 represents production cross sections measured with Be targets in this experiment, where the abscissa, Q_g^*, is the smoothed difference between the mass of the ground state of the projectile and the observed fragment, where the masses were taken from Ref. [25]. As in the previous experiment, the heaviest isotopes of elements in the middle of the distribution (Z = 19,20, 21, and 22) appear to break away from the straight-line behavior. The data were fitted by

two lines with a floating connection point, and results are shown by lines in the figure. The behavior of the slopes in the Q_g figure are summarized in Fig.6

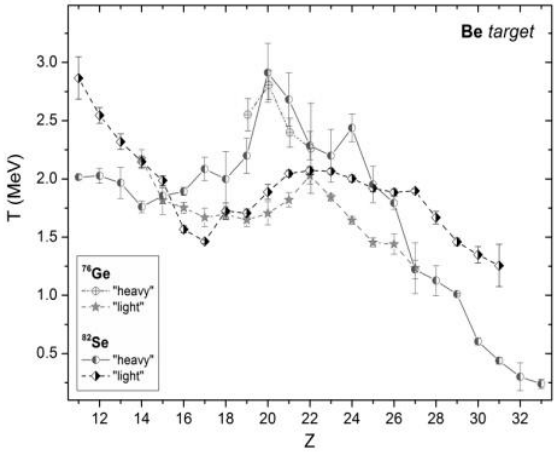

Figure 6. Values of the inverse slope parameter, *T*, from the best fit of Eq.1 to the experimental cross sections in Fig.5 shown as a function of atomic number, where half-filled green circles for heaviest isotope and half-filled black diamonds for light isotopes produced with a ^{82}Se beam on beryllium targets, whereas open magenta circles and solid brown stars for isotopes obtained with a ^{76}Ge beam [1].

.

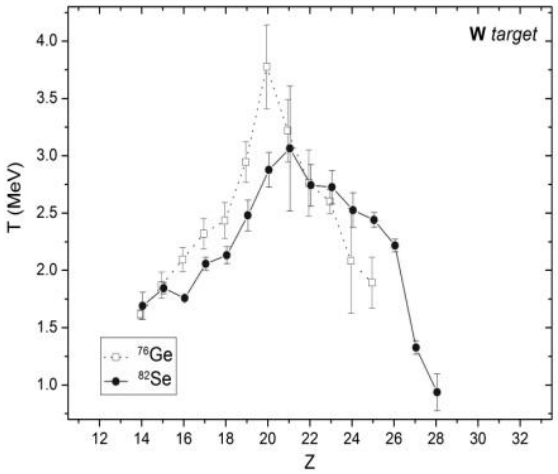

Figure 7. Similar to Fig.6 for data with the tungsten target.

where the two individual fitted values of the inverse slope parameter, *T*, for products from Be targets are shown as a function of atomic number.

The corresponding plot for the W target is shown in right Fig.7. The inverse slopes of the cross sections from the previous experiment [1] with ^{76}Ge beam are shown in these figures for comparison. Based on these figures we find that the general increase in T for all of the heavy isotopes of elements Z = 19, 20, 21, and 22 observed with a ^{76}Ge beam is reproduced by this experiment using the ^{82}Se beam, which testifies to change in the nuclear mass surface near Z = 20.

4. Production cross section for the next calcium isotopes

Based on experimental Q_g systematics (Fig.5) and the KTYU mass model [25] it is possible to extrapolate production cross sections for the next calcium isotopes with use of the ^{82}Se beam (see Fig.8).

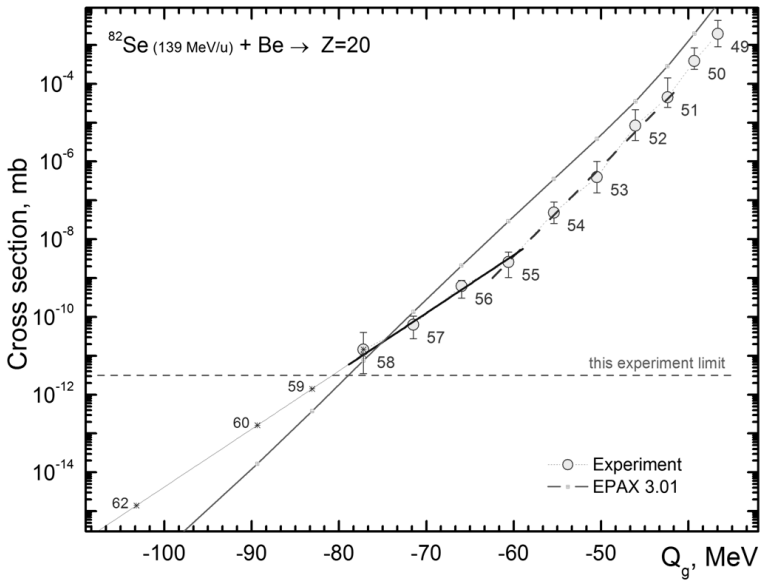

Figure 8. Experimental cross sections for the production of neutron-rich calcium isotopes, with a beryllium target as a function of Q_g-value. The solid green line corresponds to calculations by the EPAX 3.0 formula [24]. The horizontal dash line shows the limit reached in this experiment.

According to this estimation, luminosity of an experiment should be increased by factor 2.3 compared to this experiment in order to observe one event of ^{59}Ca, and by factor 20 to produce ^{60}Ca accordingly. It is important to note, that EPAX 3.01 predicts a factor of 20 less production cross section of ^{60}Ca isotope compared to the Q_g systematics.

5. Summary

The present study of the fragmentation of a ^{82}Se beam at 139 MeV/u provided evidence for the production of four previously unobserved neutron-rich isotopes. The momentum distributions and cross sections for a large number of neutron-rich nuclei produced by the ^{82}Se beam were measured by varying the target thickness in a two-stage fragment separator using a narrow momentum selection. The longitudinal momentum distributions of 122 neutron-rich isotopes of the elements with $11 \leq Z \leq 32$ were compared to models that describe the shape and centroid of fragment momentum distributions. New parameters for the semiempirical momentum distribution models [19,20] based on the measured momenta were obtained. The most neutron- rich nuclei of elements with Z = 19 to 22 were produced with an enhanced rate compared to the systematics of the production cross sections from the Q_g function. This trend was previously reported for fragmentation with ^{76}Ge beam [2], and therefore the current results confirm those of our previous experiment with a ^{76}Ge beam: a change in the nuclear mass surface near Z = 20

6. Acknowledgments

The authors would like to acknowledge the operations staff of the NSCL for developing the intense ^{82}Se beam necessary for this study. This work was supported by the U.S. National Science Foundation under grant PHY-06-06007 and PHY-11-02511.

References

1. O.B. Tarasov et al., *Phys. Rev.* **C80**, 034609 (2009).
2. O.B. Tarasov et al., *Phys. Rev. Lett.* **102**, 142501 (2009).
3. T. Baumann et al., *Nature* **449,** 1022 (2008).
4. O. B. Tarasov et al., *Phys. Rev.* **C75**, 064613 (2007).
5. P. F. Mantica et al., *Bull. Am. Phys. Soc.* **53**, 64 (2008).
6. C. Thibault et. al, *Phys. Rev.* **C76**, 644 (1975).
7. X. Campi et al., *Nucl. Phys.* **A251** 193 (1975).
8. E.K. Warburton et al., *Phys. Rev.* **C41**, 1147 (1990).
9. D. Guillemaud-Mueller et al., *Nucl. Phys.* **A426**, 37 (1984).
10. T. Motobayashi et al., *Phys. Lett.* **B346**, 9 (1995).
11. B.A. Brown, *Prog. Part. Nucl. Phys.* **47**, 517 (2001).
12. S.M. Lenzi et al., *Phys. Rev.* **C82**, 054301 (2010).
13. P. F. Mantica et al., *Phys. Rev.* **C77**, 014313 (2008).
14. M. Honma et al., *Eur. Phys. J.* **A25**, 499 (2005).
15. D. J. Morrissey et al., *Nucl. Instrum. Methods Phys. Res.* **B204**, 90 (2003).

16.D. Bazin et al., *Nucl. Instrum. Methods Phys. Res.* **B204**, 629 (2003).
17. O. B. Tarasov, D. Bazin, *Nucl. Instr. Meth. Phys. Res.* **B266**, 4657 (2008); LISE^{++} code available at: http:\\lise.nscl.msu.edu\
18. O.B.Tarasov et al., *Nucl. Instrum. Meth. Phys. Res.* **A620**, 578 (2010).
19. A.S. Goldhaber, *Phys. Lett.* **B53**, 306 (1974).
20. D. J. Morrissey, *Phys. Rev.* **C39**, **460** (1989).
21. O.B. Tarasov et al., in preparation (2013).
22. O. Tarasov, *Nucl. Phys.* **A734**, 536 (2004).
23. V. Borrel et al., *Z. Phys.* **A314**, 191 (1983).
24. K. Sümmerer, *Phys. Rev.* **C86**, 014601 (2012).
25. H. Koura et al., *Prog. Theor. Phys.* **113**, 305 (2005).